

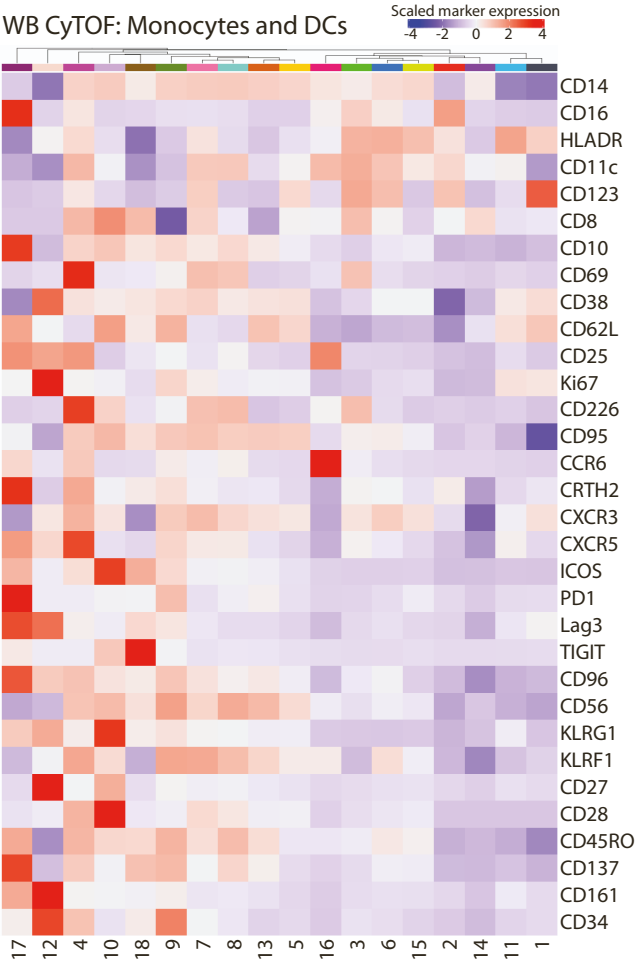
Supplemental information

**Rewired type I IFN signaling
is linked to age-dependent
differences in COVID-19**

Lev Petrov, Sophia Brumhard, Sebastian Wisniewski, Philipp Georg, David Hillus, Anna Hiller, Rosario Astaburuaga-García, Nils Blüthgen, Emanuel Wyler, Katrin Vogt, Hannah-Philine Dey, Saskia von Stillfried, Christina Iwert, Roman D. Bülow, Bruno Märkl, Lukas Maas, Christine Langner, Tim Meyer, Jennifer Loske, Roland Eils, Irina Lehmann, Benjamin Ondruschka, Markus Ralser, Jakob Trimpert, Peter Boor, Sammy Bedoui, Christian Meisel, Marcus A. Mall, Victor M. Corman, Leif Erik Sander, Jobst Röhm, and Birgit Sawitzki

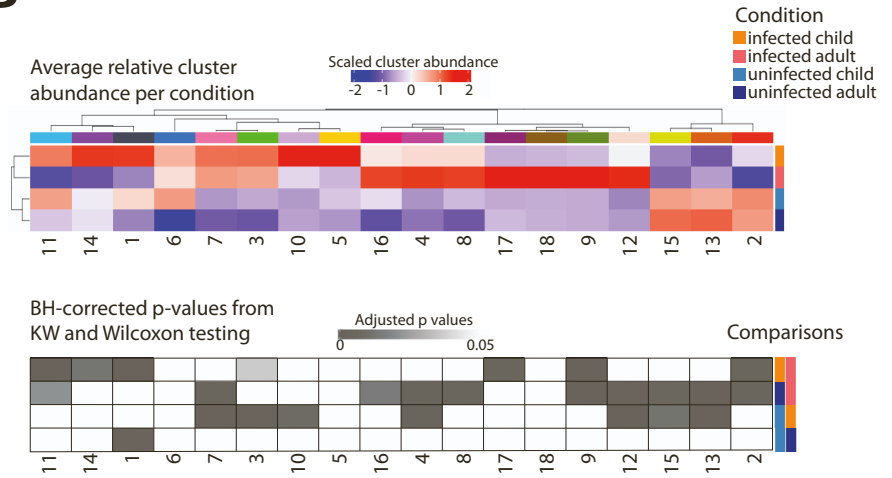


A



- 1 pDCs
- 2 non-classical
- 3 HLA-DR^{high}CD11c⁺CD69⁺ non-classical
- 4 HLA-DR^{high}CD11c⁺CD69⁺ non-classical
- 5 classical
- 6 HLA-DR^{high}CD11c⁺ intermediate
- 7 CD11c⁺CD8⁺ classical
- 8 CD11c⁺ classical
- 9 HLA-DR^{low}CD69⁺ classical
- 10 HLA-DR^{low}CD8⁺ classical
- 11 cDC
- 12 Ki67⁺ HSPC
- 13 HLA-DR^{low} classical
- 14 n.d.
- 15 HLA-DR^{high} classical
- 16 HLA-DR^{low}CD11c⁺ intermediate
- 17 n.d.
- 18 n.d.

B



C

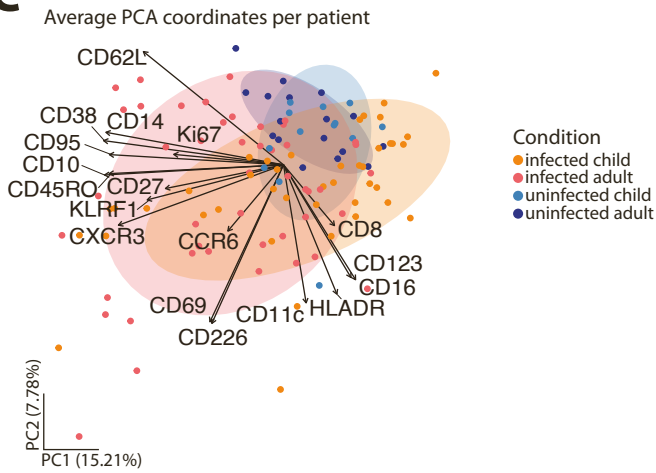


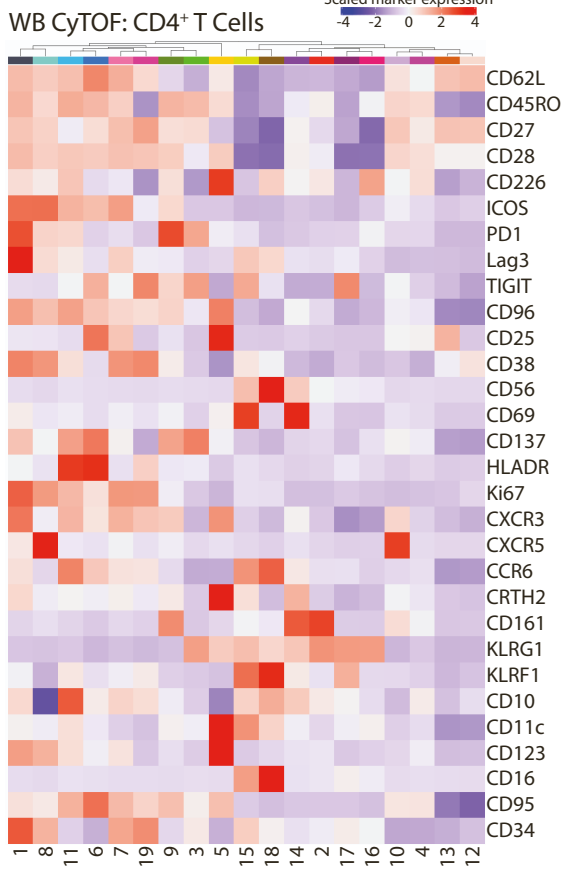
Figure S1. Annotation and statistical analysis of monocyte clusters identified by CyTOF, related to Figure 1

(A) Heatmap, containing z-score normalized average expression values of each monocyte & dendritic cell cluster resulting from a semi-supervised FlowSOM clustering approach of CyTOF data from whole blood samples (all the patients included in the dataset and used for clustering: uninfected children (RECAST n = 13; median age = 7), uninfected adults (RECAST n = 25; median age = 48), infected children (RECAST study n = 48; median age = 8; asymptomatic n = 11, symptomatic n = 37) and adults (RECAST n = 21, PA-COVID study n = 30; median age = 47; mild n = 37, severe n = 10, severe with IFN autoantibodies n = 4). The dendrogram in the upper part of the panel shows the result of distance-based hierarchical clustering. A color-coded annotation of each cluster is presented on the right, n.d. = not defined.

(B) Heatmap, showing scaled mean cluster abundance of monocyte and DC clusters for each patient group (above) and a heatmap presenting the results of statistical testing for all relevant comparisons (below; Benjamini-Hochberg-corrected p values from non-parametric Kruskal-Wallis with post-hoc Wilcoxon). Severe patients with IFN autoantibodies were excluded from the analysis.

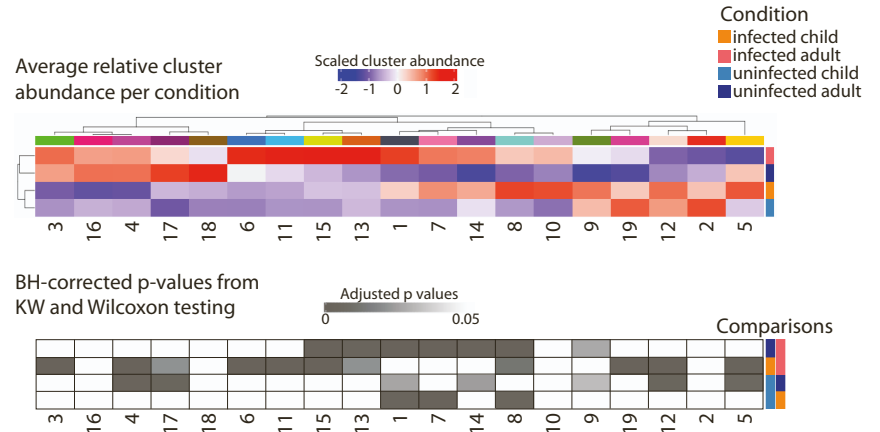
(C) PCA plot, presenting average principal component 1 and 2 coordinates of all monocyte and DC cells of each patient (colored according to patient group). The plot contains arrows labeled with marker names. These arrows represent the importance of each marker for the calculation of the components. The direction shows which principal components the marker correlates with, and the length of the arrow illustrates the magnitude of the variable's contribution to the principal components. Each arrow points in the direction where the variable it represents increases in the principal component space and longer arrows indicate that the variable has a strong influence on the principal components. Severe patients with IFN autoantibodies were excluded from the analysis.

A



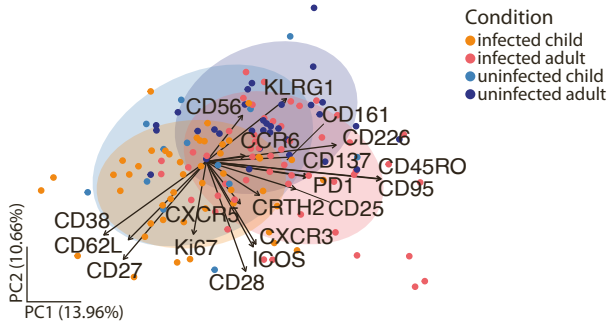
- CM 1 ICOS^{high}PD1^{high}Lag3^{high}Ki67⁺ CM 8 ICOS⁺CD38⁺CXCR5^{high}TFH-like EM 14 CD69⁺CRTH2⁺CD161^{high}
EM 2 CD226⁺CD161⁺KLRG1⁺ CM 9 ICOS⁺PD1⁺TIGIT⁺CD137⁺ TEMRA 15 Lag3⁺TIGIT⁺CD69⁺CCR6⁺CD16⁺
EM 3 PD1⁺TIGIT⁺CD137⁺ CM 10 CXCR5^{high}TFH-like TEMRA 16 CD226⁺KLRG1⁺
EM 4 CD226⁺CD96⁺CD25⁺ CM 11 TIGIT⁺CD137⁺HLA-DR⁺CCR6⁺ TEMRA 17 TIGIT⁺KLRG1⁺
CM 5 CD226^{high}CD96⁺CD25^{high}CXCR3⁺CRTH2⁺ Naive 12 CD38⁺ TEMRA 18 CD226⁺CD56^{high}NKT-like
CM 6 TIGIT⁺CD25^{high}CD137⁺HLA-DR⁺ act. Tregs Naive 13 CD25^{high}Tregs Naive 19 TIGIT⁺CD38⁺Ki67⁺CXCR3⁺
CM 7 ICOS⁺CD38⁺

B



C

Average PCA coordinates per patient



D

Intra-family comparisons

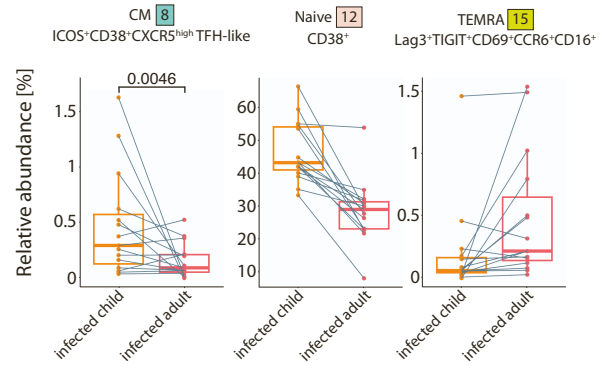


Figure S2. Annotation and statistical analysis of CD4⁺ T-cell clusters identified by CyTOF, related to Figure 2

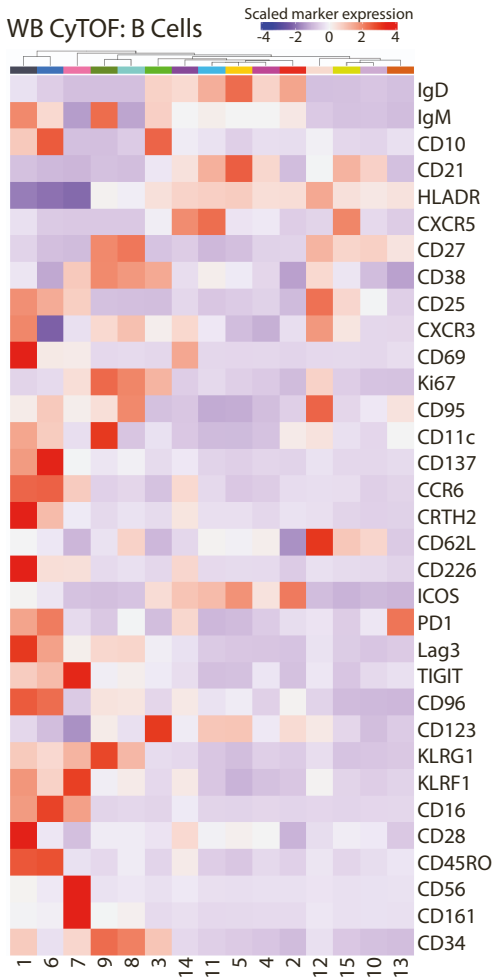
(A) Heatmap, containing z-score normalized average expression values of each CD4⁺ T-cell cluster resulting from a semi-supervised FlowSOM clustering approach of CyTOF data from whole blood samples (all the patients present in the dataset and used for clustering including follow-up measurements of some patients done approximately two weeks and six months after the first, acute infection phase measurement, were included for the heatmap calculation). Patient groups shown are: uninfected children (RECAST n = 13; median age = 7), uninfected adults (RECAST n = 25; median age = 48), infected children (RECAST study n = 53; median age = 8; asymptomatic n = 11, symptomatic n = 42) and adults (RECAST n = 24, PA-COVID study n = 51; median age = 51; mild n = 45, severe n = 24, severe with IFN autoantibodies n = 6). The dendrogram in the upper part of the panel shows the result of distance-based hierarchical clustering. A color-coded annotation of each cluster is presented on the right.

(B) Heatmap, showing scaled mean cluster abundance of CD4⁺ T-cell clusters for each patient group (above) and a heatmap presenting the results of statistical testing for all relevant comparisons (below; Benjamini-Hochberg-corrected p values from non-parametric Kruskal-Wallis with post-hoc Wilcoxon). Importantly, only samples measured during the acute phase of infection (defined as first 14 days after symptom onset) were used for calculation. Severe patients with IFN autoantibodies were excluded from the analysis. Group composition is thus as follows: uninfected children (RECAST n = 13; median age = 7), uninfected adults (RECAST n = 25; median age = 48), infected children (RECAST study n = 48; median age = 8; asymptomatic n = 11, symptomatic n = 37) and adults (RECAST n = 21, PA-COVID study n = 26; median age = 45; mild n = 37, severe n = 10).

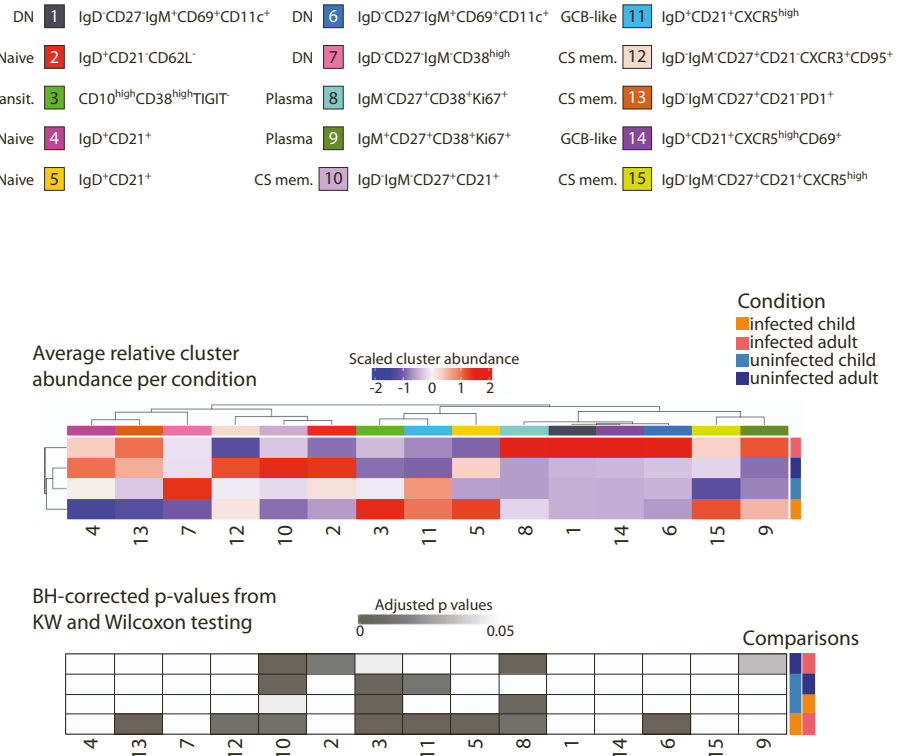
(C) PCA plot, presenting average principal component 1 and 2 coordinates of all CD4⁺ T cells of each patient (colored according to patient group). The plot contains arrows labeled with marker names. These arrows represent the importance of each marker for the calculation of the components. The direction shows which principal components the marker correlates with and the length of the arrow illustrates the magnitude of the variable's contribution to the principal components. Simply put, each arrow points in the direction where the variable it represents increases in the principal component space and longer arrows indicate that the variable has a strong influence on the principal components. Severe patients with IFN autoantibodies were excluded from the analysis.

(D) Box plots, showing relative frequencies of annotated clusters, resulting from the FlowSOM algorithm, applied to the CD4⁺ T-cell CyTOF data. Cluster abundance is compared between infected children (RECAST study n = 20; median age = 9; asymptomatic n = 3, symptomatic n = 17) and infected adults (RECAST study n = 19; median age = 39; mild n = 19) within the same family. Abundances were averaged, if multiple parents (mother and father) or children were measured in a family (family n = 15). Lines connect parents and children from the same family. Only samples measured during the acute phase of infection (defined as first 14 days after symptom onset) are shown. Statistical testing was done using pairwise Wilcoxon rank sum test.

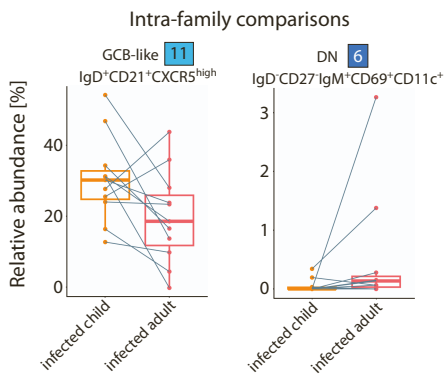
A



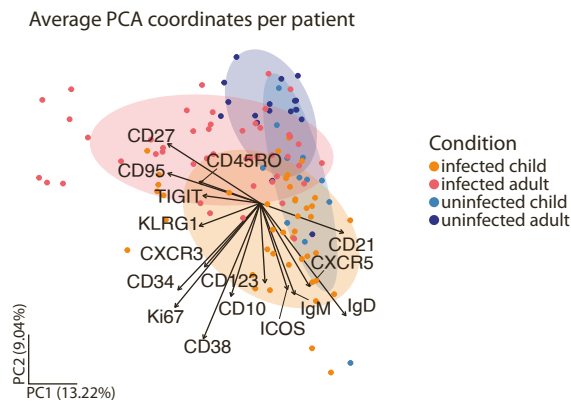
B



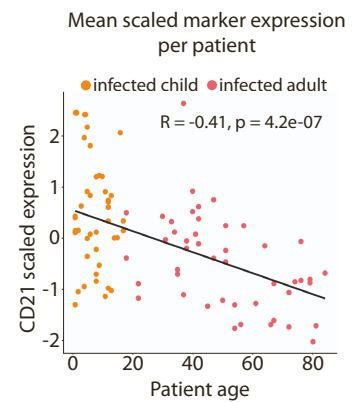
C



D



E



F

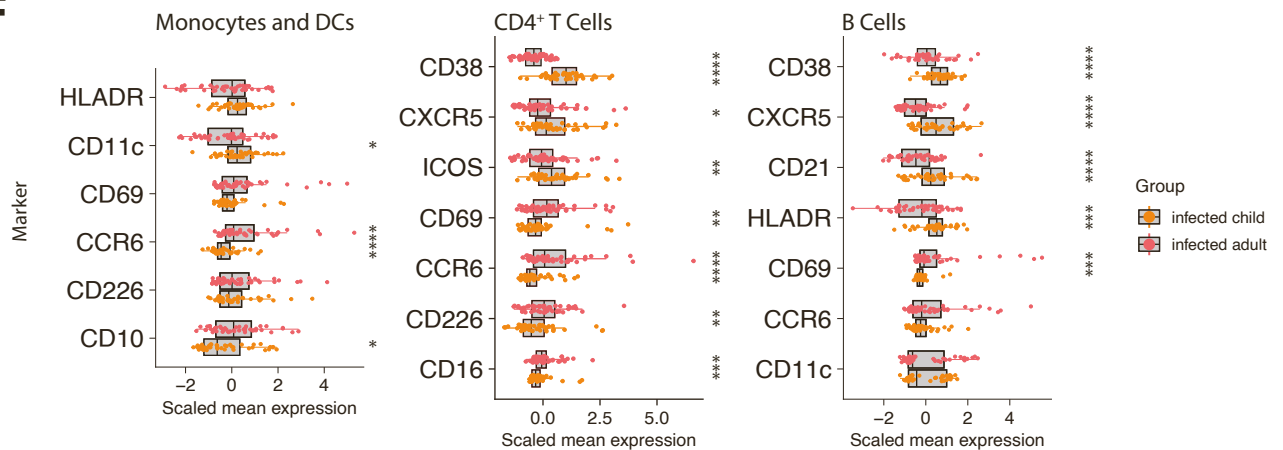


Figure S3. Annotation and statistical analysis of B-cell clusters identified by CyTOF, common cross-leukocyte pattern of age-dependency in infection-induced activation marker expression, related to Figure 2

(A) Heatmap, containing z-score normalized average expression values of each B-cell cluster resulting from a semi-supervised FlowSOM clustering approach of CyTOF data from whole blood samples (all the patients included in the dataset and used for clustering: uninfected children (RECAST n = 13; median age = 7), uninfected adults (RECAST n = 25; median age = 48), infected children (RECAST study n = 48; median age = 8; asymptomatic n = 11, symptomatic n = 37) and adults (RECAST n = 21, PA-COVID study n = 30; median age = 47; mild n = 37, severe n = 10, severe with IFN autoantibodies n = 4)). The dendrogram in the upper part of the panel shows the result of distance-based hierarchical clustering. A color-coded annotation of each cluster is presented on the right.

(B) Heatmap, showing scaled mean cluster abundance of B-cell clusters for each patient group (above) and a heatmap presenting the results of statistical testing for all relevant comparisons (below; Benjamini-Hochberg-corrected p values from non-parametric Kruskal-Wallis with post-hoc Wilcoxon). Severe patients with IFN autoantibodies were excluded from the analysis.

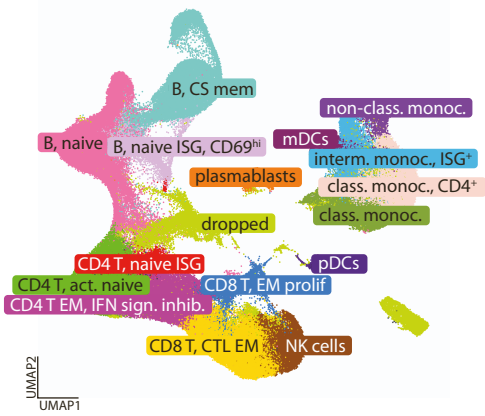
(C) Box plots, showing relative frequencies of annotated clusters, resulting from the FlowSOM algorithm, applied to the B-cell CyTOF data. Cluster abundance is compared between infected children (RECAST study n = 16; median age = 9; asymptomatic n = 2, symptomatic n = 14) and infected adults (RECAST study n = 14; median age = 38; mild n = 14) within the same family. Abundances were averaged, if multiple parents (mother and father) or children were measured in a family (family n = 11). Lines connect parents and children from the same family. Statistical testing was done using pairwise Wilcoxon rank sum test.

(D) PCA plot, presenting average principal component 1 and 2 coordinates of all B cells of each patient (colored according to patient group). The plot contains arrows labeled with marker names. These arrows represent the importance of each marker for the calculation of the components. The direction shows which principal components the marker correlates with and the length of the arrow illustrates the magnitude of the variable's contribution to the principal components. Simply put, each arrow points in the direction where the variable it represents increases in the principal component space and longer arrows indicate that the variable has a strong influence on the principal components. Severe patients with IFN autoantibodies were excluded from the analysis.

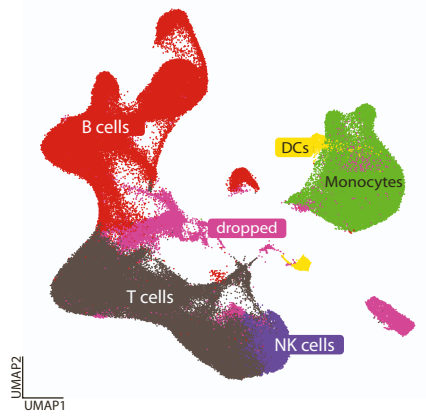
(E) Scatter plot, showing mean z-score normalized CD21 expression in relationship to patient age for infected patients (linear model fitted to data and Spearman's rank correlation coefficient shown in black) within B-cell CyTOF data. Severe patients with IFN autoantibodies were excluded from the analysis.

(F) Box plots, showing mean z-score normalized expression per patient for a curated list of markers for monocytes and DCs, CD4⁺ T cells and B cells. Signals are compared between infected children (RECAST study n = 48; median age = 8; asymptomatic n = 11, symptomatic n = 37) and adults (RECAST n = 21, PA-COVID study n = 26; median age = 45; mild n = 37, severe n = 10). Wilcoxon; *, p < 0.05; **, p < 0.01; ***, p < 0.001; ****, p < 0.0001.

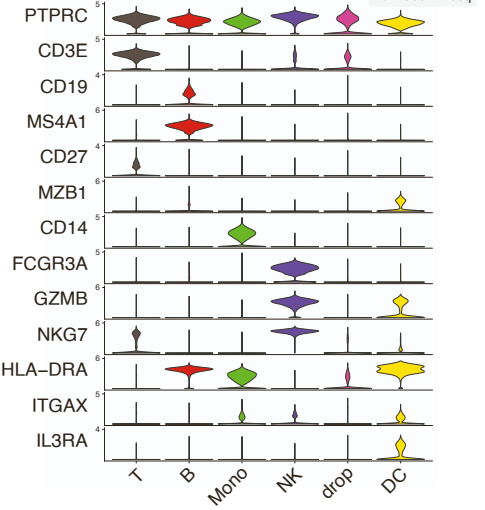
A

PBMC scRNAseq: Annotation
217,193 cells

B

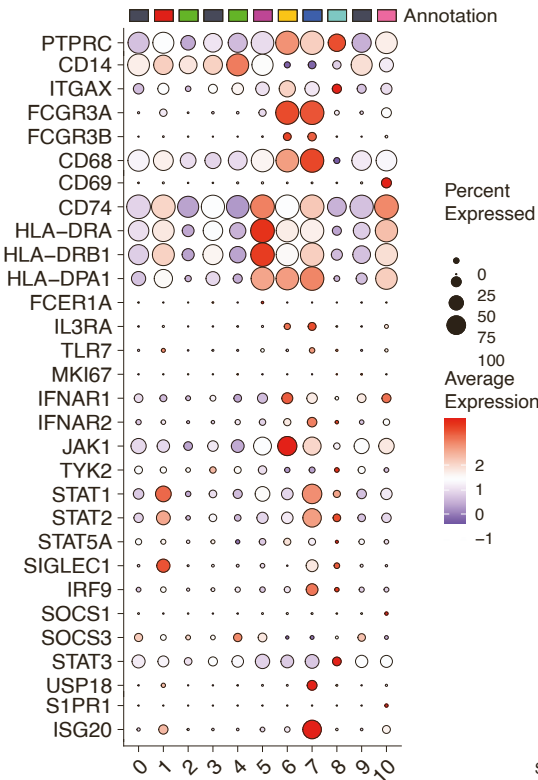
PBMC scRNAseq: Subsetting
217,193 cells

C

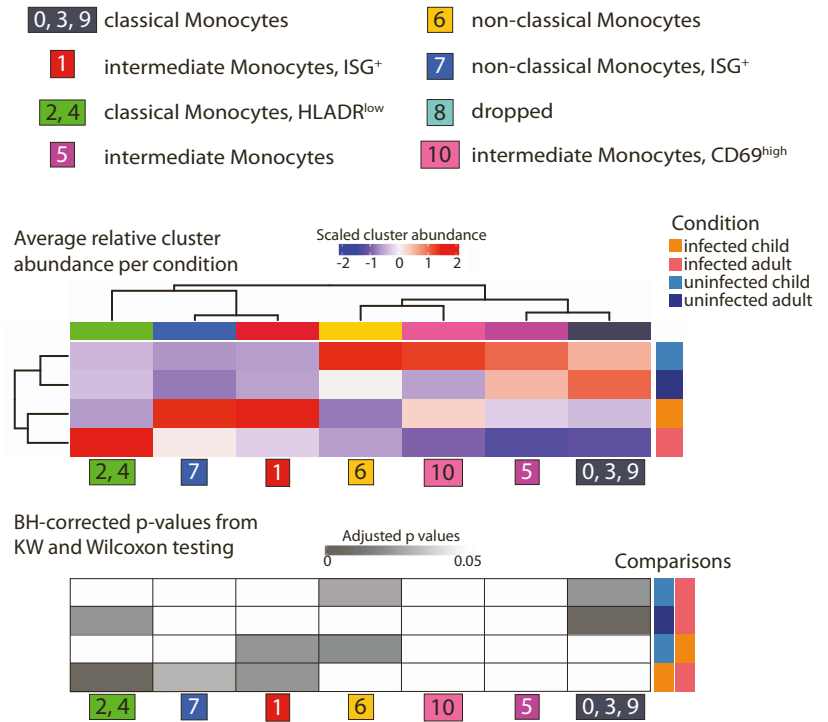


D

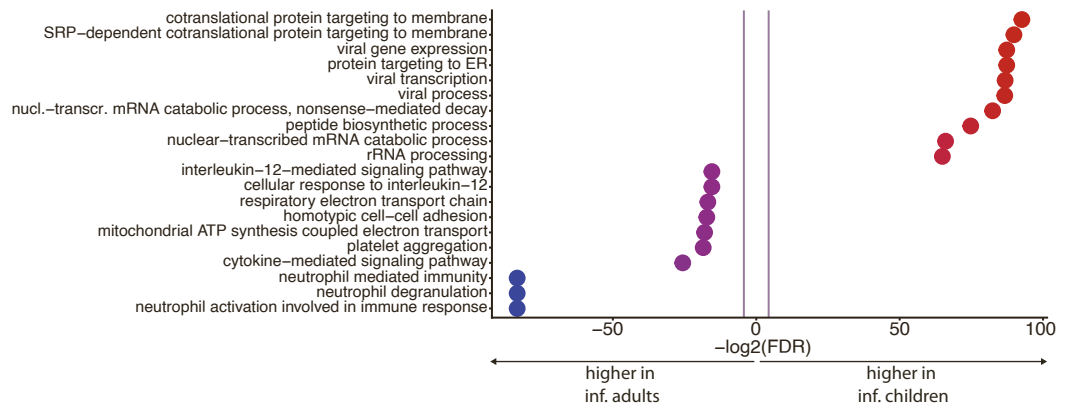
PBMC scRNAseq: Monocytes



E



F



G

Concentration of cytokines in serum of infected patients

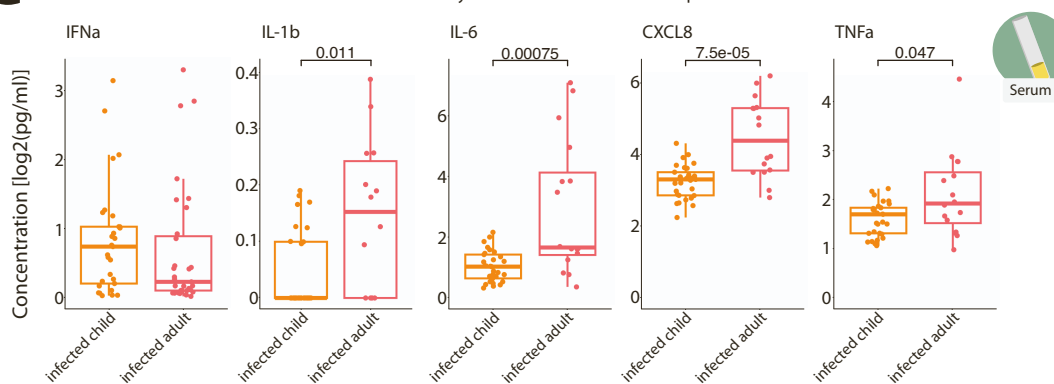


Figure S4. scRNAseq-based molecular profiling of circulating monocytes and cytokine concentrations in serum of infected patients point at increased inflammatory state in infected adults, related to Figure 3

(A) UMAP representation of the total PBMC scRNAseq data. 26 clusters have been produced using a graph-based approach as implemented in Seurat package (KNN graph with Louvain community detection). Clusters were then annotated based on the expression of the most commonly used marker genes of immune metapopulations. UMAP presents all the patients included in the dataset and used for clustering: uninfected children (RECAST study n = 5; median age = 7), uninfected adults (RECAST study n = 4, EICOV/COVIMMUNIZE study n = 4; median age = 66), infected children (RECAST study n = 13; median age = 9; asymptomatic n = 5, symptomatic n = 8) and infected adults (RECAST study n = 1; PA-COVID study n = 18; median age = 67; mild n = 5, severe n = 7, severe with IFN autoantibodies n = 7).

(B) UMAP representation of the total PBMC scRNAseq data. 26 annotated clusters from S3A were assigned a metapopulation tag, based on the expression of the most commonly used marker genes. These tags were then used for splitting the dataset into DC, monocyte, NK, T and B-cell subsets, which were then separately subclustered to achieve a more granular resolution. Clusters that were either a mix of different immune cell lineages or did not have a high enough PTPRC gene expression were annotated as “dropped” and excluded from further analysis.

(C) Violin plots, showing some of the marker genes used for the annotation of the metapopulations.

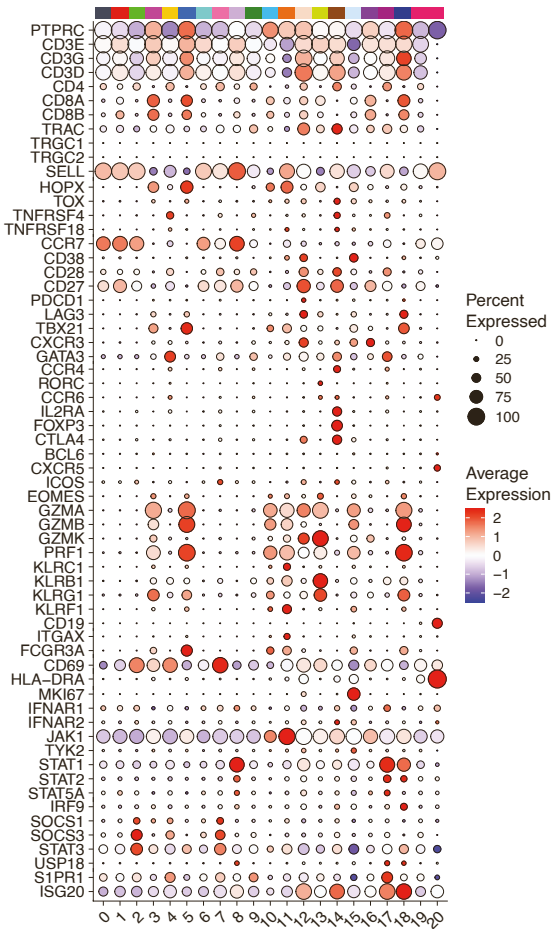
(D) Dotplot, showing average scaled expression of a curated, subset defining list of genes for monocyte cells, subset from the PBMC scRNAseq data. 11 clusters have been produced using a graph-based approach as implemented in Seurat package (KNN graph with Louvain community detection). Some clusters share annotation due to phenotypical similarity and accumulation pattern and are treated as one population for abundance testing in S3E. Annotations of the clusters are shown on the right-hand side from the dotplot. The cluster annotated as “dropped” was of low quality (as concluded from inspecting number of features, n of counts and percentage of mitochondrial genes as well as other population-specific genes). The dotplot presents all the patients included in the dataset and used for clustering: uninfected children (RECAST study n = 5; median age = 7), uninfected adults (RECAST study n = 4, EICOV/COVIMMUNIZE study n = 4; median age = 66), infected children (RECAST study n = 13; median age = 9; asymptomatic n = 5, symptomatic n = 8) and infected adults (RECAST study n = 1; PA-COVID study n = 18; median age = 67; mild n = 5, severe n = 7, severe with IFN autoantibodies n = 7).

(E) Heatmap, showing scaled mean cluster abundance of monocyte clusters for each patient group (above) and a heatmap presenting the results of statistical testing for all relevant comparisons (below; Benjamini-Hochberg-corrected p values from non-parametric Kruskal-Wallis with post-hoc Wilcoxon). Severe patients with IFN autoantibodies were excluded from the analysis.

(F) Gene set enrichment analysis (GSEA) applied to monocytes from the PBMC scRNAseq experiment and clusters, expanded with infection (1, 4 and 7). GSEA was done using the 189 significantly differentially expressed genes from the infected adults – infected children comparison, shown in volcano plot F3D. R interface EnrichR was used to access Enrichr "GO Biological Process 2018" database for automatic annotation of enriched gene sets. Severe patients with IFN autoantibodies were excluded from the analysis.

(G) Box plots of selected pro-inflammatory cytokines' serum concentrations in infected patients (inf. children RECAST study n = 29; median age = 9; asymptomatic n = 9, symptomatic n = 20; inf. adults RECAST study n = 5, PA-COVID study n = 26; median age = 54; mild n = 12, severe n = 14). Median DPSO in infected children = 5.5, median DPSO in infected adults = 9. Wilcoxon p values shown.

A

PBMC scRNAseq: TCRab⁺ T Cells0 CD4⁺, naive 11 CD4⁺/CD8⁺ naive2 CD4⁺, naive STAT3^{high}, SOCS3^{high}3 CD8⁺, GZMK^{high} CX3CR1^{low} CTL4 CD4⁺, EM TNFRSF4⁺5 CD8⁺, GZMK^{low} CX3CR1^{high} CTL6 CD4⁺, naive 27 CD4⁺, CM STAT3^{high}, SOCS3^{high}8 CD4⁺, naive ISG⁺9 CD4⁺, CM GATA3⁺10 CD8⁺, EM11 CD8⁺, CM12 CD4⁺/CD8⁺ PD1^{high}13 CD8⁺, KLRB1^{high} MAIT14 CD4⁺ Tregs15 CD4⁺/CD8⁺ EM MKI67⁺16 CD8⁺, EM CXCR3^{high}17 CD4⁺, CM GATA3⁺, ISG⁺18 CD8⁺, EM ISG⁺

19, 20 dropped

Condition

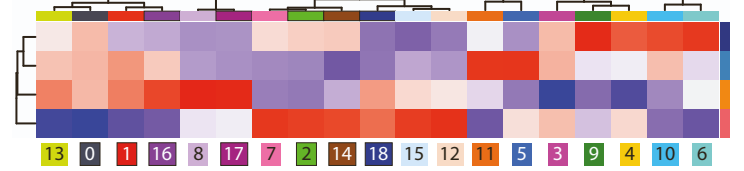
infected child
infected adult
uninfected child
uninfected adult

B

Average relative cluster abundance per condition

Scaled cluster abundance

-2 -1 0 1 2



BH-corrected p-values from KW and Wilcoxon testing

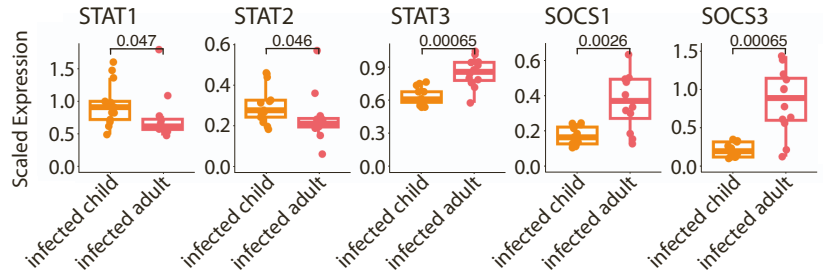
Adjusted p values

0 0.05

Comparisons

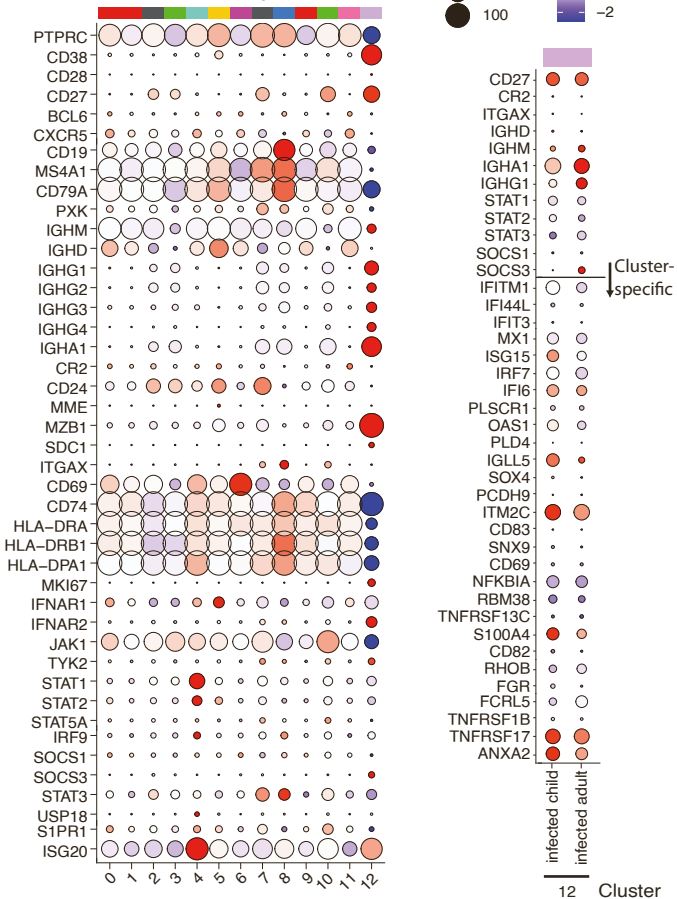


C



D

PBMC scRNAseq: B Cells



0, 1, 9 naive B

2, 7 CS mem B

3, 10 CS mem B, TCF7⁺4 naive B, ISG⁺

5 transitional B

6 DN-like, activated, CD69^{high}

8 DN B cells

11 dropped

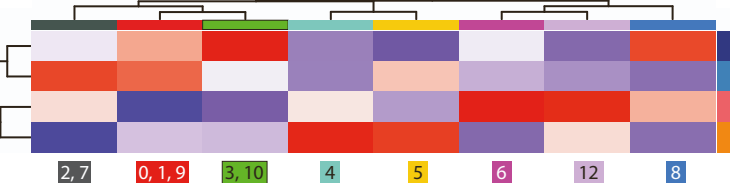
12 plasmablasts

E

Average relative cluster abundance per condition

Scaled cluster abundance

-2 -1 0 1 2



BH-corrected p-values from KW and Wilcoxon testing

Adjusted p values

0 0.05

Comparisons

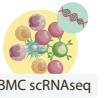
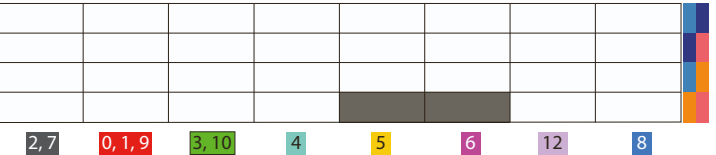


Figure S5. scRNAseq profiling of TCRab⁺ T-cell and B-cell space, related to Figure 4

(A) Dotplot, showing average scaled expression of a curated, subset defining list of genes for TCRab⁺ T cells, subset from the PBMC scRNAseq data. 21 clusters have been produced using a graph-based approach as implemented in Seurat package (KNN graph with Louvain community detection). Annotations of the clusters are shown on the right-hand side from the dotplot. Clusters annotated as “dropped” were of low quality (as concluded from inspecting number of features, n of counts and percentage of mitochondrial genes as well as other population-specific genes). The dotplot presents all the patients included in the dataset and used for clustering: uninfected children (RECAST study n = 5; median age = 7), uninfected adults (RECAST study n = 4, EICOV/COVIMMUNIZE study n = 4; median age = 66), infected children (RECAST study n = 13; median age = 9; asymptomatic n = 5, symptomatic n = 8) and infected adults (RECAST study n = 1; PA-COVID study n = 18; median age = 67; mild n = 5, severe n = 7, severe with IFN autoantibodies n = 7).

(B) Heatmap, showing scaled mean cluster abundance of TCRab⁺ T-cell clusters for each patient group (above) and a heatmap presenting the results of statistical testing for all relevant comparisons (below; Benjamini-Hochberg-corrected p values from non-parametric Kruskal-Wallis with post-hoc Wilcoxon). Severe patients with IFN autoantibodies were excluded from the analysis.

(C) Box plots, showing mean scaled expression of selected genes, involved in IFN signaling, calculated over all TCRab⁺ T cells from clusters expanded with infection (2, 7, 8, 12, 15, 16, 17 and 18) for infected children (RECAST study n = 13; median age = 9; asymptomatic n = 5, symptomatic n = 8) and infected adults (RECAST study n = 1; PA-COVID study n = 11; median age = 63.5; mild n = 5, severe n = 7). Wilcoxon p values shown.

(D) Left hand side: dotplot, showing average scaled expression of a curated, subset defining list of genes for B cells, subset from the PBMC scRNAseq data. 13 clusters have been produced using a graph-based approach as implemented in Seurat package (KNN graph with Louvain community detection). Annotations of the clusters are shown on the right-hand side from the dotplot. Cluster annotated as “dropped” was of low quality (as concluded from inspecting number of features, n of counts and percentage of mitochondrial genes as well as other population-specific genes). The dotplot presents all the patients included in the dataset and used for clustering: uninfected children (RECAST study n = 5; median age = 7), uninfected adults (RECAST study n = 4, EICOV/COVIMMUNIZE study n = 4; median age = 66), infected children (RECAST study n = 13; median age = 9; asymptomatic n = 5, symptomatic n = 8) and infected adults (RECAST study n = 1; PA-COVID study n = 18; median age = 67; mild n = 5, severe n = 7, severe with IFN autoantibodies n = 7). Right hand side: Dotplot, showing scaled average expression of genes in cluster 12, split by infected patient group. Severe patients with IFN autoantibodies were excluded from the analysis. A horizontal line splits the dotplot in two parts – genes above the line were curated based on the presence of clusters with pronounced ISG signature and include other genes useful for annotation, genes below the line were found to be differentially expressed between the clusters (FindMarkers Seurat function).

(E) Heatmap, showing scaled mean cluster abundance of B-cell clusters for each patient group (above) and a heatmap presenting the results of statistical testing for all relevant comparisons (below; Benjamini-Hochberg-corrected p values from non-parametric Kruskal-Wallis with post-hoc Wilcoxon). Severe patients with IFN autoantibodies were excluded from the analysis.

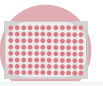
Figure S6. Age-dependent activation profiles are not driven by comorbidities and can be confirmed in a hamster infection model, related to Figure 5

(A) Left hand side: dotplot, showing TCRab⁺ cells, subset from the nasal swab scRNAseq data.⁸ 8 clusters have been produced using a graph-based approach as implemented in Seurat package (KNN graph with Louvain community detection). Annotations of the clusters are shown on the right-hand side from the dotplot. The dotplot presents all the patients included in the dataset and used for clustering: uninfected children (RECAST study n = 18; median age = 9), uninfected adults (RECAST study n = 23; median age = 46), infected children (RECAST study n = 24; median age = 9; asymptomatic n = 2, symptomatic n = 22) and infected adults (RECAST study n = 21; median age = 39; mild n = 21). Patients with DPSO range from 0 to 12 days were included (inf. children mean = 4.5, inf. adult mean = 5). Right hand side: dotplot, showing scaled average expression of genes in cluster 7, split by infected patient group. Severe patients with IFN autoantibodies were excluded from the analysis. A horizontal line splits the dotplot in two parts – genes above the line were curated based on the presence of clusters with pronounced ISG signature and include other genes useful for annotation, genes below the line were found to be differentially expressed between the clusters (FindMarkers Seurat function).

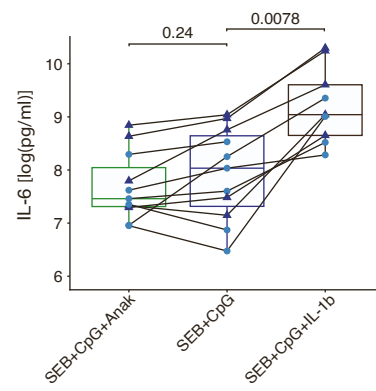
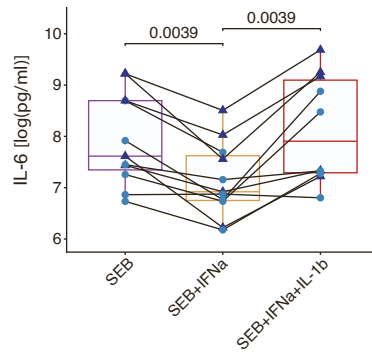
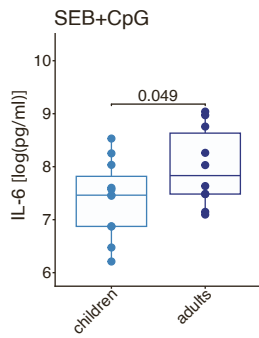
(B) Heatmap, showing scaled mean cluster abundance of TCRab⁺ cell clusters for each patient group (above) and a heatmap presenting the results of statistical testing for all relevant comparisons (below; Benjamini-Hochberg-corrected p values from non-parametric Kruskal-Wallis with post-hoc Wilcoxon).

(C) Scatterplots, illustrating the results of modelling dependency between age and mean z-score normalized CD38 and CCR6 expression by CD4⁺ T cells or CXCR5 and CD69 expression by B cells from the CyTOF experiment together with Charlson Comorbidity Index (CCI, w/o age factor) and obesity (as binary variable, 1 if BMI > 30). Light green line shows the impact of CCI and obesity on the intercept value of the model (intercept + CCI coefficient + obesity coefficient). CCI score was calculated excluding age, as age is already present in the model as a separate variable. Distance between the two lines thus represents the influence of the CCI score and obesity on the intercept (mean value of the response variable when all the predictor variables are zero). Obesity status is marked by triangular shape of a point, comorbidity by a light green fill. Figure annotation includes the respective coefficients and p values as modelled with linear regression. Infected children (RECAST study n = 48; median age = 8; asymptomatic n = 11, symptomatic n = 37) and adults (RECAST n = 21, PA-COVID study n = 26; median age = 45; mild n = 37, severe n = 10) are shown.

(D) Heatmaps, summarizing the differential gene expression analysis results of gene sets identified to be up-regulated in infection-induced leukocyte populations (in human PBMC scRNAseq data) determined by bulk RNA sequencing of whole blood samples collected at day 2 after infection from young (n=3, 6 weeks old) and old (n=3, 32-34 weeks old) hamsters (left side) as well as uninfected controls (n=3, right side, 6 weeks old).

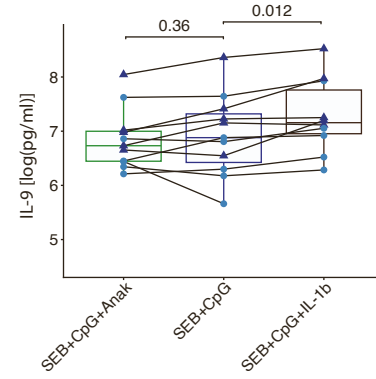
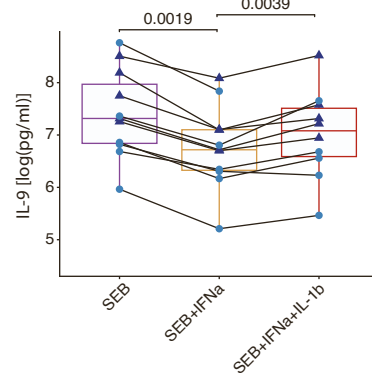
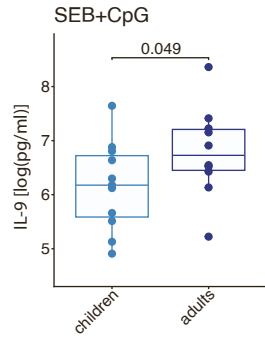


IFN α and IL-1 β dependency of IL-6 concentration in supernatant



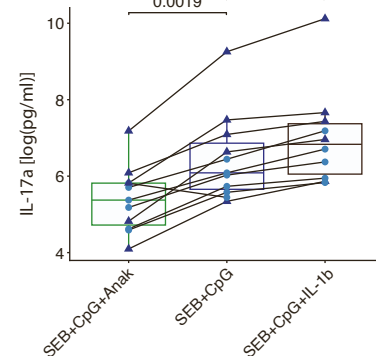
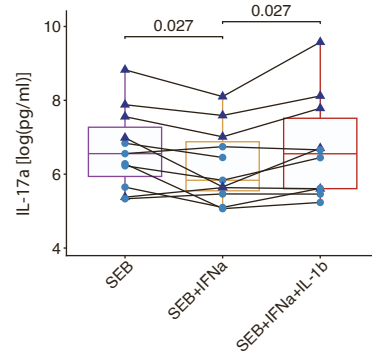
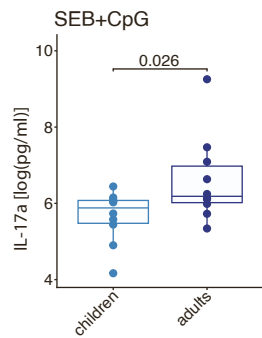
Group
● children
▲ adults

IFN α and IL-1 β dependency of IL-9 concentration in supernatant



Group
● children
▲ adults

IFN α and IL-1 β dependency of IL-17a concentration in supernatant



Group
● children
▲ adults

Figure S7. IL-1b-mediated interference with type I IFN signaling explains enhanced cytokine production potential of adult leukocytes, related to Figure 6

Box plots showing the difference in IL-6, IL-9 and IL-17A release between the two age groups when stimulated by SEB and CpG (first column from the left; uninfected children, RECAST study n = 11; median age = 9; uninfected adult, RECAST study n = 10; median age = 55; one-sided Wilcoxon p value shown), or by different combinations of SEB, CpG, recombinant IFN α (0.5ng/ml), IL-1b and IL-1b inhibitor Anakinra (uninfected children, RECAST study n = 6; median age = 8; uninfected adults, RECAST study n = 5; median age = 55; p values shown for paired Wilcoxon test, adjusted with Hommel procedure).

Table S2: Cohort summary and statistics, related to all Figures.				
	Uninfected children	Uninfected adults	Infected children	Infected adults
Total number	22	49	58	98
- RECAST	22	35	58	40
- PA-COVID	0	0	0	58
- COVIMMUNIZE, EICOV	0	14	0	0
Age, median (range)	8.5 (2–16)	52 (25-86)	8 (1-17)	47 (18-84)
Sex				
- Male, N (%)	10 (45%)	24 (49%)	30 (52%)	51 (52%)
- Female, N (%)	12 (55%)	25 (51%)	28 (48%)	47 (48%)
COVID-19, WHO scale, N (%)				
- Asymptomatic (1)	0 (0%)	0 (0%)	11 (19%)	0 (0%)
- Mild (2-4)	0 (0%)	0 (0%)	47 (81%)	68 (69%)
- Severe (5-8)	0 (0%)	0 (0%)	0 (0%)	30 (31%)
DPSO first visit, median±SD, mean (range)	n/a	n/a	4.5±3.3 5 (-1-11)	8±4.5 7.7 (-3-19)
DPSO second visit, median±SD, mean (range)	n/a	n/a	20±3.8 20 (12-30)	22±5.3 22 (12-41)
DPSO third visit, median±SD, mean (range)	n/a	n/a	147±16.2 153 (129-183)	181±26.4 176 (122-245)
CCI w/o age factor > 0, N (%), median CCI w/o age factor (range)	0 (0%) 0 (n/a)	9 (18.4%) 0 (0-4)	2 (3.5%) 0 (0-1)	30 (30.6%) 0 (0-7)
- Myocardial infarction, N (%)	0 (0%)	0 (0%)	0 (0%)	3 (3.1%)
- Chronic heart failure, N (%)	0 (0%)	0 (0%)	0 (0%)	0 (0%)
- Peripheral artery disease, N (%)	0 (0%)	1 (2%)	0 (0%)	2 (2%)
- Cerebrovascular accident / transient ischemic stroke, N (%)	0 (0%)	2 (4.1%)	0 (0%)	1 (1%)
- Dementia, N (%)	0 (0%)	1 (2%)	0 (0%)	0 (0%)
- Chronic obstructive pulmonary disease, N (%)	0 (0%)	2 (4.1%)	0 (0%)	7 (7.1%)
- Connective tissue disorder, N (%)	0 (0%)	2 (4.1%)	0 (0%)	2 (2%)
- Peptic ulcer disease, N (%)	0 (0%)	0 (0%)	0 (0%)	0 (0%)
- Chronic liver disease, N (%)	0 (0%)	0 (0%)	0 (0%)	4 (4.1%)
- Diabetes, N (%)	0 (0%)	0 (0%)	2 (3.5%)	17 (17.3%)
- Chronic kidney disease, N (%)	0 (0%)	0 (0%)	0 (0%)	6 (6.1%)
- Tumor, N (%)	0 (0%)	5 (10.2%)	0 (0%)	3 (3.1%)
- Leukaemia, N (%)	0 (0%)	0 (0%)	0 (0%)	0 (0%)
- Lymphoma, N (%)	0 (0%)	0 (0%)	0 (0%)	0 (0%)
- AIDS, N (%)	0 (0%)	0 (0%)	0 (0%)	1 (1%)
Other COVID-relevant comorbidities				
- Asthma, N (%)	1 (4.5%)	3 (6.1%)	1 (1.7%)	5 (5.1%)
- Obesity, N (%) *only 40 uninf. adult patients with BMI available	1 (4.5%)	2 (4.1%)*	1 (1.7%)	23 (23.5%)

Table S3: Patient kinship annotation for intra-family comparisons, related to Figures S2D, S3C.

patient_id	family_id	category
468	1	adult
471	1	child
481	2	adult
482	2	adult
483	2	child
50001	3	child
50004	3	adult
50005	4	child
50006	4	child
50007	4	adult
50017	5	adult
50019	5	child
50026	6	child
50050	7	adult
50051	7	child
50053	7	adult
50057	8	child
50058	8	adult
50108	9	child
50110	9	adult
50126	10	child
50128	10	adult
50129	10	adult
50134	11	adult
50135	11	adult
50136	11	child
50137	11	child
50138	12	adult
50139	12	adult
50140	12	child
50143	13	adult
50144	13	child
50165	14	adult
50166	14	child
50170	15	child
50171	15	child
50172	15	child
50174	15	adult
50181	16	adult
50182	16	child
50183	16	child